

# Exact probability distribution for the two-tag displacement in single-file motion

Sanjib Sabhapandit<sup>1</sup> and Abhishek Dhar<sup>2</sup>

<sup>1</sup>Raman Research Institute, Bangalore - 560080, India

<sup>2</sup>International centre for theoretical sciences, TIFR, Bangalore - 560012, India

**Abstract.** We consider a gas of point particles moving on the one-dimensional line with a hard-core inter-particle interaction that prevents particle crossings — this is usually referred to as single-file motion. The individual particle dynamics can be arbitrary and they only interact when they meet. Starting from initial conditions such that particles are uniformly distributed, we observe the displacement of a tagged particle at time  $t$ , with respect to the initial position of *another* tagged particle, such that their tags differ by  $r$ . For  $r = 0$ , this is the usual well studied problem of the tagged particle motion. Using a mapping to a non-interacting particle system we compute the exact probability distribution function for the two-tagged particle displacement, for general single particle dynamics. As by-products, we compute the large deviation function, various cumulants and, for the case of Hamiltonian dynamics, the two-particle velocity auto-correlation function.

PACS numbers: 05.40.-a, 83.50.Ha, 87.16.dp, 05.60.Cd

## 1. Introduction

Starting with the pioneering work of Jepsen [1] and Harris [2], the study of tagged particle motion has been an area of very active research. Much of the earlier studies focused [3, 4, 5, 6, 7, 8, 9, 10, 11, 12, 13, 14, 15, 16, 17, 18, 19, 20] on the statistics of the typical displacement of the tagged particle, in particular on the mean square displacement in various single-file systems. One of the most interesting result is that, for a Hamiltonian one-dimensional gas of hard particles which move ballistically between elastic collisions, a tagged particle moves *diffusively*, thus the mean square displacement of the tagged particle, in a time duration  $t$  increases as  $\langle X_t^2 \rangle \sim t$ . On the other hand, for a gas of Brownian particles with hard-core interactions, the tagged particle motion is *sub-diffusive*, with  $\langle X_t^2 \rangle \propto t^{1/2}$ . The typical fluctuations of the tagged particle displacement is described by a Gaussian distribution with the above variance. Recently there has been interest in studying the probability of *atypical* fluctuations of the tagged particle displacement [21, 22, 23, 24]. Some of the results for these simple classical interacting particle models have been useful in obtaining results for one-dimensional quantum systems [25, 26].

A number of different theoretical approaches have been used to study the probability distribution of the tagged particle displacement. These include the original ideas of Jepsen and Harris of mapping to a non-interacting system, exact solution of multi-particle Fokker-Planck equation with reflecting boundary condition between neighboring particles, and the recently developed approach of Macroscopic fluctuation theory. In our recent works [16, 22], we have shown a simpler way (as opposed to earlier approaches in [1, 3, 4]) of using the non-interacting picture to computing tagged particle statistics. In the present work, we extend this method to study a particular two particle distribution, defined below.

We consider a hard-point particle system on the infinite line. The particles are distributed uniformly with a finite density  $\rho$ . For the case of Hamiltonian dynamics (of equal mass particles), the initial velocities are taken to be independent and identically distributed random variables. The particles move ballistically in between elastic binary collisions. During collisions, the two colliding particles merely interchange their velocities. As a result, any set of particle trajectories of the interacting system can be constructed from the set of trajectories of a non-interacting system (where the trajectories pass through each other) — by exchanging the identities (tags) of the particles at crossing. For the case of Brownian particles with hard-point interactions, Harris [2] defined the interacting particle problem by starting with the non-interacting trajectories and exchanging particle identities whenever two trajectories cross. This definition is equivalent to enforcing reflecting boundary conditions between nearest neighbor pairs in the full multi-particle propagator (thus each particle acts like a hard reflecting wall for its nearest neighbors).

One can generalize this collision rule to other cases where the individual particle dynamics is neither Hamiltonian or Brownian, for example Lèvy walks or fractional

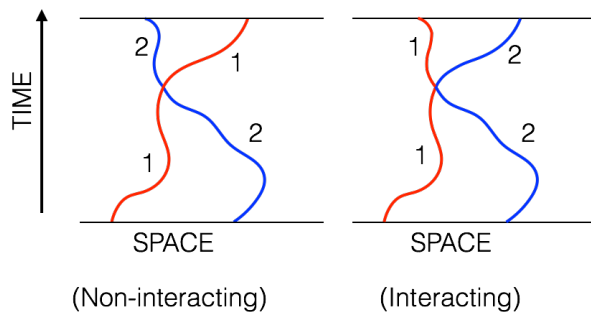


**Figure 1.** (Color online) An interacting hard-point particles system can be constructed from a non-interacting system by exchanging tags (colors) when two trajectories cross.

Brownian motion. Hence in general we define the interacting problem as follows: start with the non-interacting trajectories and interchange particle labels whenever two trajectories cross.

For this general interacting particle system, let us tag two particles with tag indices 0 and  $r$ , such that there are  $r - 1$  particles in between them. Let the position of these particles be  $x_0(t)$  and  $x_r(t)$  respectively. Here we consider the displacement  $X_t = x_r(t) - x_0(0)$  and compute its statistics.

## 2. Main steps of the calculation

Initially, we consider  $2N + 1$  particles, independently and uniformly distributed in the interval  $[-L, L]$  and evolve them on the infinite one dimensional line. Since during a collision each particle acts as a reflecting hard wall for the other and the particles are identical, one can effectively treat the system of the interacting hard-point particles as non-interacting by exchanging the identities of the particles emerging from collisions [see figure 1 and discussion in previous section]. In the non-interacting picture, each particle executes an independent motion and the particles *pass through each other* when they ‘collide’. The position of each particle at time  $t$  is given independently by a single-particle propagator of the general form

$$G(y, t|x, 0) = \frac{1}{\sigma_t} f\left(\frac{y - x}{\sigma_t}\right), \quad (1)$$

where  $f(-w) = f(w) \geq 0$  and  $\langle |y - x| \rangle / \sigma_t = \int_{-\infty}^{\infty} |w| f(w) dw = \Delta$  is finite. Evidently,  $\int_{-\infty}^{\infty} f(w) dw = 1$ . The dependence on time only appears through the characteristic displacement  $\sigma_t$  in time  $t$ . While for stochastic processes the propagator arises naturally, for Hamiltonian systems (where the dynamics is deterministic) it comes from the distribution, taken to be of the form  $\bar{v}^{-1} f(v/\bar{v})$ , from which the initial velocities of the particles are chosen independently. In many problems of interest, the propagator happens to be Gaussian, i.e.,  $f(x) = e^{-x^2/2} / \sqrt{2\pi}$ , and  $\sigma_t^2$  is the variance. For example, for Brownian particles,  $\sigma_t = \sqrt{2Dt}$ , where  $D$  is the diffusion coefficient, while for

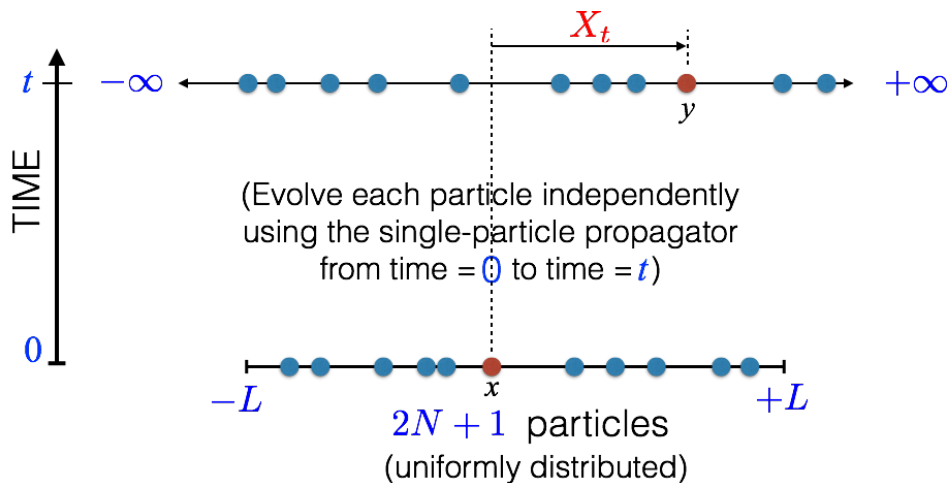


**Figure 2.** We mark the position by  $x = x_j(0)$  of the  $j^{\text{th}}$  particle at  $t = 0$  and the position  $y = x_k(t)$  of the  $k^{\text{th}}$  particle at time  $t$ . In this example,  $j = 6$  and  $k = 9$ . The variable  $X_t = y - x$  denotes the displacement of the  $k^{\text{th}}$  particle at time  $t$  with respect to the initial position of the  $j^{\text{th}}$  particle.

Hamiltonian dynamics with Gaussian velocity distribution we have  $\sigma_t = \bar{v}t$ . Similarly for fractional Brownian motion,  $\sigma_t \propto t^H$ , where  $H$  is the Hurst exponent. However, our analysis is valid for any general propagator. Note that the dependence on time only appears through the characteristic displacement  $\sigma_t$  in time  $t$ .

We mark the position  $x = x_j(0)$  of the  $j^{\text{th}}$  particle at  $t = 0$  and the position  $y = x_k(t)$  of the  $k^{\text{th}}$  particle at time  $t$  [see figure 2]. Let  $X_t = y - x$ , be the difference between these two positions. Our goal is to study the statistical properties of this random variable  $X_t$ , in the thermodynamic limit  $N \rightarrow \infty$ ,  $L \rightarrow \infty$  while keeping  $N/L = \rho$  fixed. In this limit, in the bulk, the statistics of  $X_t$  should depend only on the difference of the tags  $r = k - j$ , rather than the individual tags  $j$  and  $k$ . Therefore, we set  $j = N + 1$  (the middle particle) and  $k = N + 1 + r$  ( $r^{\text{th}}$  particle counted from the middle particle) before taking the thermodynamic limit. In the thermodynamic limit,  $X_t$  denotes the displacement of a particle at time  $t$ , with respect to the initial position of *another* particle such that their tags differ by  $r$ . For  $r = 0$ , this represents the usual problem of tagged particle displacement, studied in [22].

In the following we proceed with the calculation using the non-interacting picture discussed above.

### 2.1. The joint PDF of two particles

The joint probability density function (PDF)  $P(x, j, 0; y, k, t)$  of the  $j^{\text{th}}$  particle being at  $x$  at time  $t = 0$ , and the  $k^{\text{th}}$  particle being at  $y$  at time  $t$ , can be expressed in terms of properties of the non-interacting particles. In the non-interacting picture, there are two possibilities: (i) the  $j^{\text{th}}$  particle at time  $t = 0$  becomes the  $k^{\text{th}}$  particle at time  $t$ , (ii) a second particle becomes the  $k^{\text{th}}$  particle at time  $t$  [see figure 3]. We need to sum

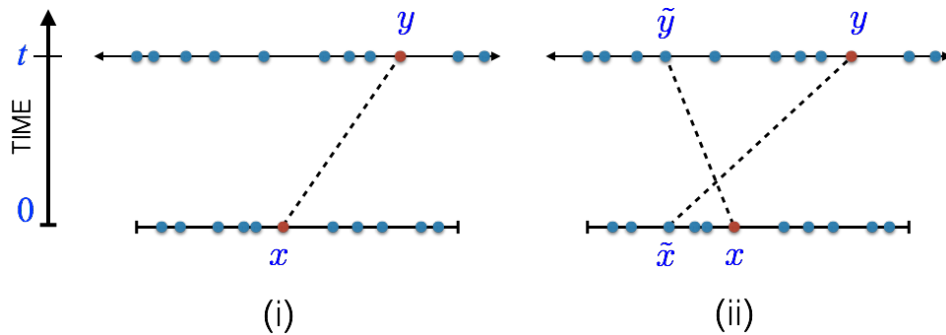


**Figure 3.** In the non-interacting picture, there are two possibilities: (i) the  $j^{\text{th}}$  particle at time  $t = 0$  becomes the  $k^{\text{th}}$  particle at time  $t$ , (ii) a second particle becomes the  $k^{\text{th}}$  particle at time  $t$ . For the case (ii) there are four situations (a)  $\tilde{x} < x$  and  $\tilde{y} < y$ , (b)  $\tilde{x} > x$  and  $\tilde{y} > y$ , (c)  $\tilde{x} < x$  and  $\tilde{y} > y$ , and (d)  $\tilde{x} > x$  and  $\tilde{y} < y$  respectively.

over these two processes to get,

$$P(x, j, 0; y, k, t) = P_{(1)}(x, j, 0; y, k, t) + P_{(2)}(x, j, 0; y, k, t), \quad (2)$$

where  $P_{(1)}$  and  $P_{(2)}$  are the joint PDFs corresponding to the processes (i) and (ii) respectively.

To compute the contribution from process (i) we pick one of the non-interacting particles at random at time  $t = 0$ , multiply by the propagator [given in (1)] that it goes from  $(x, 0)$  to  $(y, t)$ , and then multiply by the probability that it is the  $j^{\text{th}}$  particle at  $t = 0$  and the  $k^{\text{th}}$  particle at time  $t$ . Thus we obtain the corresponding joint PDF as

$$P_{(1)}(x, j, 0; y, k, t) = \frac{(2N+1)}{2L} G(y, t|x, 0) F_{1N}(x, j, y, k, t), \quad (3)$$

where  $F_{1N}(x, j, y, k, t)$  is the probability that there are  $(j-1)$  particles to the left of  $x$  at  $t = 0$  and  $(k-1)$  particles to the left of  $y$  at  $t$ .

To compute the contribution from process (ii), we first pick two particles at random at time  $t = 0$ , and multiply by the propagators that they go from  $(x, 0)$  to  $(\tilde{y}, t)$  and  $(\tilde{x}, 0)$  to  $(y, t)$  respectively. We then multiply by the probability there are an  $(j-1)$  particles on the left of  $x$  at time  $t = 0$  and  $(k-1)$  particles to the left of  $y$  at  $t$ . Finally, integrating with respect to  $\tilde{x}, \tilde{y}$ , we get the joint PDF corresponding to this process as

$$P_{(2)}(x, j, 0; y, k, t) = \frac{(2N+1)(2N)}{(2L)^2} \int_{-L}^L d\tilde{x} \int_{-\infty}^{\infty} d\tilde{y} G(\tilde{y}, t|x, 0) G(y, t|\tilde{x}, 0) F_{2N}(x, j, y, k, \tilde{x}, \tilde{y}, t), \quad (4)$$

where  $F_{2N}(x, j, y, k, \tilde{x}, \tilde{y}, t)$  is the probability that there are  $(j-1)$  particles on left of  $x$  at  $t = 0$  and  $(k-1)$  particles on the left of  $y$  at time  $t$ , given that there is a particle at  $\tilde{x}$  at time  $t = 0$ , and a particle at  $\tilde{y}$  at time  $t$ .

To proceed further, we need the expressions for  $F_{1N}$  and  $F_{2N}$ . Let  $p_{-+}(x, y, t)$  be the probability that a particle is to the left of  $x$  at  $t = 0$  and to the right of  $y$  at time  $t$ .

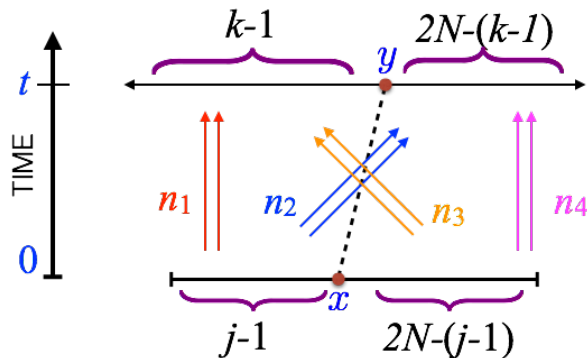


**Figure 4.** A particle goes from the initial position  $x$  to the position  $y$  in time  $t$ .  $n_1$  denotes the number of particles going from the left of  $x$  to the left of  $y$ ,  $n_2$  denotes the number of particles going from left of  $x$  to the right of  $y$ ,  $n_3$  denotes the number of particles going from the right of  $x$  to the left of  $y$ , and  $n_4$  denotes the number of particles going from the right of  $x$  to the right of  $y$ , and  $n_1 + n_2 + n_3 + n_4 = 2N$ . There are  $j - 1$  particles on the left of  $x$  at  $t = 0$  and  $k - 1$  particles on the left of  $y$  at time  $t$ .

Similarly, we define the other three complementary probabilities. Clearly,

$$p_{-+}(x, y, t) = (2L)^{-1} \int_{-L}^x dx' \int_y^{\infty} dy' G(y', t|x', 0), \quad (5a)$$

$$p_{+-}(x, y, t) = (2L)^{-1} \int_x^L dx' \int_{-\infty}^y dy' G(y', t|x', 0), \quad (5b)$$

$$p_{--}(x, y, t) = (2L)^{-1} \int_{-L}^x dx' \int_{-\infty}^y dy' G(y', t|x', 0), \quad (5c)$$

$$p_{++}(x, y, t) = (2L)^{-1} \int_x^L dx' \int_y^{\infty} dy' G(y', t|x', 0), \quad (5d)$$

and  $p_{++} + p_{+-} + p_{-+} + p_{--} = 1$ . Armed with the above four probabilities, we now evaluate  $F_{1N}$  and  $F_{2N}$  below.

## 2.2. Evaluation of $F_{1N}(x, j, y, k, t)$

In this case, out of  $2N + 1$  particles, the  $j^{\text{th}}$  particle at the initial time goes from the position  $x$  to the position  $y$  in time  $t$  and becomes the  $k^{\text{th}}$  particle at the final time. The remaining  $2N$  particles are independent of each other and the selected particle. Let  $n_1$  be the number of particles going from the left of  $x$  to the left of  $y$ ,  $n_2$  be the number of particles going from left of  $x$  to the right of  $y$ ,  $n_3$  be the number of particles going from the right of  $x$  to the left of  $y$ , and  $n_4$  be the number of particles going from the right of  $x$  to the right of  $y$  [see figure 4]. Clearly  $n_1 + n_2 + n_3 + n_4 = 2N$ . Moreover, since there are  $j - 1$  particles on the left of  $x$ , clearly,  $n_1 + n_2 = j - 1$  and  $n_3 + n_4 = 2N - (j - 1)$ . Similarly, since there are  $k - 1$  particles on the left of  $y$ , we have  $n_1 + n_3 = k - 1$  and  $n_2 + n_4 = 2N - (k - 1)$ . These equalities imply  $n_4 - n_1 = 2N + 2 - k - j$  and  $n_3 - n_2 = k - j$ .

The number of ways of choosing the set  $\{n_1, n_2, n_3, n_4\}$  is given by the multinomial coefficient

$$\frac{(2N)!}{n_1!n_2!n_3!n_4!},$$

and each possibility occurs with probability  $p_{--}^{n_1}p_{-+}^{n_2}p_{+-}^{n_3}p_{++}^{n_4}$ . Hence, summing over all possible values of  $\{n_1, n_2, n_3, n_4\}$  we get

$$F_{1N} = \sum_{n_1+n_2+n_3+n_4=2N} \frac{(2N)!}{n_1!n_2!n_3!n_4!} p_{--}^{n_1}p_{-+}^{n_2}p_{+-}^{n_3}p_{++}^{n_4} \delta[n_4-n_1-2N-2+k+j] \delta[n_3-n_2-k+j], \quad (6)$$

where  $\delta[n]$  is the Kronecker delta function:  $\delta[n] = 1$  if  $n = 0$  and  $\delta[n] = 0$  for  $n \neq 0$ . Now, after using the integral representation of the Kronecker delta,

$$\delta[m-n] = \frac{1}{2\pi} \int_{\theta_0}^{\theta_0+2\pi} e^{i(m-n)\theta} d\theta \quad (\text{where the initial phase } \theta_0 \text{ is arbitrary}), \quad (7)$$

in the above equation, it immediately follows that

$$F_{1N}(x, i, y, j, t) = \int_{\phi_0}^{\phi_0+2\pi} \frac{d\phi}{2\pi} \int_{\theta_0}^{\theta_0+2\pi} \frac{d\theta}{2\pi} [H(x, y, \theta, \phi, t)]^{2N} e^{-i\phi(2N+2-k-j)} e^{-i\theta(k-j)}, \quad (8)$$

where

$$H(x, y, \theta, \phi, t) = p_{++}(x, y, t)e^{i\phi} + p_{--}(x, y, t)e^{-i\phi} + p_{+-}(x, y, t)e^{i\theta} + p_{-+}(x, y, t)e^{-i\theta} \quad (9a)$$

$$= 1 - (1 - \cos \phi) (p_{++} + p_{--}) + i \sin \phi (p_{++} - p_{--}) \\ - (1 - \cos \theta) (p_{+-} + p_{-+}) + i \sin \theta (p_{+-} - p_{-+}). \quad (9b)$$

Now, using the fact that  $2N$  is even and the above integral remains unchanged if both  $\phi$  and  $\theta$  are shifted by  $\pi$  simultaneously, the range of the  $\phi$  integral has been broken into two parts and each of these contributes equally. After appropriately choosing the initial phases, this gives,

$$F_{1N}(x, y, t) = \int_{-\pi/2}^{\pi/2} \frac{d\phi}{\pi} \int_{-\pi}^{\pi} \frac{d\theta}{2\pi} [H(x, y, \theta, \phi, t)]^{2N} e^{-i\phi(2N+2-k-j)} e^{-i\theta(k-j)}. \quad (10)$$

### 2.3. Evaluation of $F_{2N}(x, j, y, k, \tilde{x}, \tilde{y}, t)$

In this case a particle whose initial tag is different from  $j$ , goes from  $\tilde{x}$  to  $y$  and becomes the  $k^{\text{th}}$  particle at time  $t$ , while the initial  $j^{\text{th}}$  particle goes from  $x$  to  $\tilde{y}$  in time  $t$  whose final tag is different from  $k$ . To compute  $F_{2N}$ , one has to keep track of both these particles. Apart from these two particles, let there be  $n_1$  particles going from the left of  $x$  to the left of  $y$ ,  $n_2$  particles going from the left of  $x$  to the right of  $y$ ,  $n_3$  particles going from the right of  $x$  to the left of  $y$ , and  $n_4$  particles going from the right of  $x$  to the right of  $y$ . Since two of the particles are considered separately, the rest can be chosen in  $(2N-1)!/(n_1!n_2!n_3!n_4!)$  different ways and  $n_1 + n_2 + n_3 + n_4 = 2N - 1$ . The other two constraints among  $\{n_i\}$ 's are given by  $n_4 - n_1 = 2N + 2 - k - j + \chi_1$  and  $n_3 - n_2 = k - j + \chi_2$ . Unlike the previous case where  $\chi_1 = \chi_2 = 0$ , here their values depend on the order of the positions  $(x, \tilde{x})$  and  $(y, \tilde{y})$ . There arises four situations:

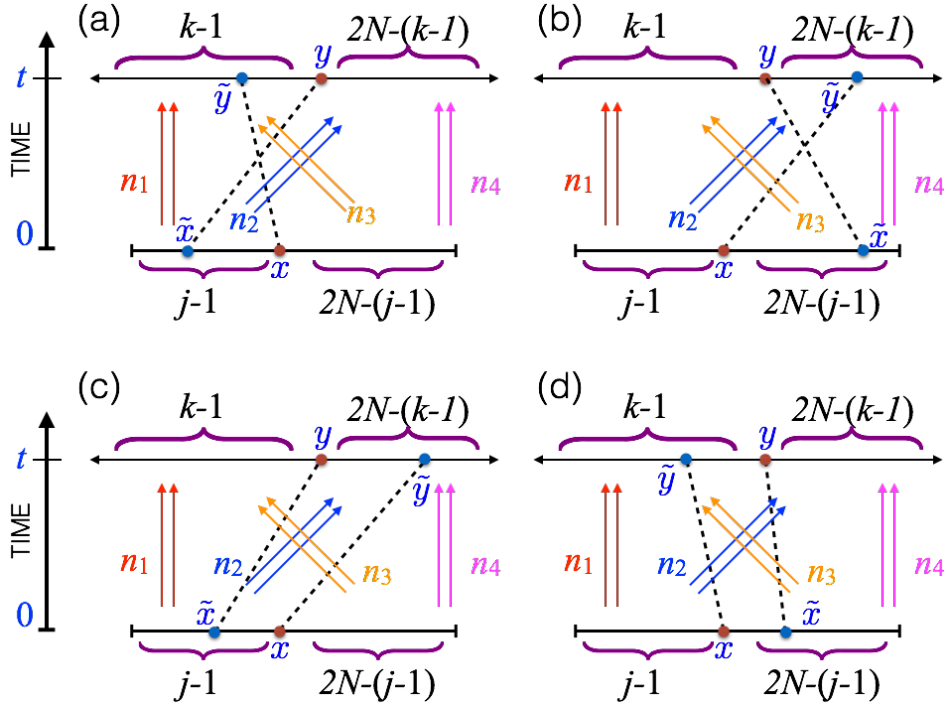


**Figure 5.** A particle goes from the initial position  $x$  to the position  $\tilde{y}$  in time  $t$ , while at the same time, another particle from its initial position  $\tilde{x}$  goes to  $y$ .  $n_1$  denotes the number of particles going from the left of  $x$  to the left of  $y$ ,  $n_2$  denotes the number of particles going from left of  $x$  to the right of  $y$ ,  $n_3$  denotes the number of particles going from the right of  $x$  to the left of  $y$ , and  $n_4$  denotes the number of particles going from the right of  $x$  to the right of  $y$ , and  $n_1 + n_2 + n_3 + n_4 = 2N - 1$ . There are  $j - 1$  particles on the left of  $x$  at  $t = 0$  and  $k - 1$  particles on the left of  $y$  at time  $t$ .

- (a)  $\tilde{x} < x$  and  $\tilde{y} < y$ , for which  $\chi_1 = 1$  and  $\chi_2 = 0$ ,
- (b)  $\tilde{x} > x$  and  $\tilde{y} > y$ , for which  $\chi_1 = -1$  and  $\chi_2 = 0$ ,
- (c)  $\tilde{x} < x$  and  $\tilde{y} > y$ , for which  $\chi_1 = 0$  and  $\chi_2 = 1$ ,
- (d)  $\tilde{x} > x$  and  $\tilde{y} < y$ , for which  $\chi_1 = 0$  and  $\chi_2 = -1$ .

Now following the procedure used to evaluate  $F_{1N}$ , it is easily found that case, one has to keep track of the

$$F_{2N}(x, y, \tilde{x}, \tilde{y}, t) = \int_{-\pi/2}^{\pi/2} \frac{d\phi}{\pi} \int_{-\pi}^{\pi} \frac{d\theta}{2\pi} [H(x, y, \theta, \phi, t)]^{2N-1} e^{-i\phi(2N+2-k-j)} e^{-i\theta(k-j)} e^{-i\phi\chi_1} e^{-i\theta\chi_2}. \quad (11)$$

#### 2.4. Exact PDF of the two-tag displacement in the thermodynamic limit

So far our calculations are exact, valid for any  $N$  and  $L$ . We now assume both  $N$  and  $L$  to be large and keep only the dominant terms. Finally, we will take the thermodynamic limit  $N \rightarrow \infty$ ,  $L \rightarrow \infty$  while keeping  $N/L = \rho$  fixed. We now set  $k = j + r$  and  $j = N + 1$ . We also change our notation to  $P_{(1)}(x, N + 1, 0; y, N + 1 + r, t) \rightarrow P_{(1)}(x, y, r, t)$ ,



$P_{(2)}(x, N + 1, 0; y, N + 1 + r, t) \rightarrow P_{(2)}(x, y, r, t)$  and

$$P(x, y, r, t) = P_{(1)}(x, y, r, t) + P_{(2)}(x, y, r, t). \quad (12)$$

From (3) and (10) we get

$$P_{(1)}(x, y, r, t) = \frac{\rho}{\sigma_t} f(z) \int_{-\pi/2}^{\pi/2} \frac{d\phi}{\pi} \int_{-\pi}^{\pi} \frac{d\theta}{2\pi} [H(x, y, \theta, \phi, t)]^{2N} e^{i\phi r} e^{-i\theta r}, \quad (13)$$

where  $z = (y - x)/\sigma_t$ . Similarly from (4) and (11) and performing the integration over  $\tilde{x}$  and  $\tilde{y}$ , we get

$$P_{(2)}(x, y, r, t) = \rho^2 \int_{-\pi/2}^{\pi/2} \frac{d\phi}{\pi} \int_{-\pi}^{\pi} \frac{d\theta}{2\pi} [H(x, y, \theta, \phi, t)]^{2N-1} e^{i\phi r} e^{-i\theta r} \\ \times [2A_1(z)A_2(z) \cos \phi + A_1^2(z)e^{-i\theta} + A_2^2(z)e^{i\theta}], \quad (14)$$

where the functions  $A_{1,2}(z)$  are given by

$$A_1(z) = \int_{\sigma_t z}^{\infty} G(x, t|0, 0) dx = \int_z^{\infty} f(w) dw, \quad \text{and} \quad A_2(z) = 1 - A_1(z). \quad (15)$$

Now we explicitly compute the expressions for  $p_{\pm\pm}$  using (1). Keeping only the dominant terms up to  $O(1/L)$ , which survive in the limit  $N \rightarrow \infty$ ,  $L \rightarrow \infty$  while keeping  $N/L = \rho$  fixed, we get

$$p_{-+} = \frac{\sigma_t}{2L} \left[ -\frac{z}{2} + Q(z) \right] + \dots \quad (16a)$$

$$p_{+-} = \frac{\sigma_t}{2L} \left[ \frac{z}{2} + Q(z) \right] + \dots \quad (16b)$$

$$p_{--} = \frac{1}{2} + \frac{\sigma_t}{2L} \left[ \frac{\bar{z}}{2} - Q(z) \right] + \dots \quad (16c)$$

$$p_{++} = \frac{1}{2} + \frac{\sigma_t}{2L} \left[ -\frac{\bar{z}}{2} - Q(z) \right] + \dots, \quad (16d)$$

where  $z = (y - x)/\sigma_t$ ,  $\bar{z} = (y + x)/\sigma_t$ , and

$$Q(z) = z \int_0^z f(w) dw + \int_z^{\infty} w f(w) dw. \quad (17)$$

Now, substituting  $p_{\pm\pm}$  in the expression (9b), for large  $N$ , keeping only the most dominant terms, one finds

$$H^{2N} = e^{-2N(1-\cos \phi)} e^{-i\rho\sigma_t \bar{z} \sin \phi} e^{-2\rho\sigma_t Q(z)(1-\cos \theta)} e^{i\rho\sigma_t z \sin \theta}. \quad (18)$$

The PDF of  $X_t = y - x$  is given by

$$P_{\text{tag}}(X_t, r, t) = \int_{-\infty}^{\infty} \int_{-\infty}^{\infty} \delta(X_t - [y - x]) P(x, y, r, t) dx dy. \quad (19)$$

Using (18), in (12)–(14), and making a change of variables from  $x, y$  to  $z, \bar{z}$ , we can finally write down the above PDF of  $X_t$  as

$$P_{\text{tag}}(X_t = \sigma_t z, r, t) = \lim_{N \rightarrow \infty} \int_{-\infty}^{\infty} \frac{d\bar{z}}{2} \int_{-\pi/2}^{\pi/2} \frac{d\phi}{\pi} \int_{-\pi}^{\pi} \frac{d\theta}{2\pi} \rho B(z, \theta, \phi) \\ \times e^{-2N(1-\cos\phi)} e^{-i\rho\sigma_t \bar{z} \sin\phi} e^{-2\rho\sigma_t Q(z)(1-\cos\theta)} e^{i\rho\sigma_t z \sin\theta} e^{i\phi r} e^{-i\theta r}, \quad (20)$$

where  $B(z, \theta, \phi) = f(z) + \rho\sigma_t [2A_1(z)A_2(z)\cos\phi + A_1^2(z)e^{-i\theta} + A_2^2(z)e^{i\theta}]$ . For large  $N$ , the major contribution of the integral over  $\phi$  comes from the region around  $\phi = 0$ . Therefore, the  $\phi$  integral can be performed by expanding around  $\phi = 0$  to make it a Gaussian integral (while extending the limits to  $\pm\infty$ ). Subsequently, one can also perform the Gaussian integral over  $\bar{z}$ . This leads to the exact expression,

$$P_{\text{tag}}(X_t = \sigma_t z, r, t) = \frac{1}{\sigma_t} \int_{-\pi}^{\pi} \frac{d\theta}{2\pi} B(z, \theta) e^{-\rho\sigma_t [2Q(z)(1-\cos\theta) - iz \sin\theta]} e^{-i\theta r}, \quad (21)$$

where

$$B(z, \theta) \equiv B(z, \theta, 0) = f(z) + \rho\sigma_t [2A_1(z)A_2(z) + A_1^2(z)e^{-i\theta} + A_2^2(z)e^{i\theta}]. \quad (22)$$

In fact, using the integral representation of the modified Bessel function of the first kind, for integer order  $n$ ,

$$I_n(x) = \int_{-\pi}^{\pi} \frac{d\theta}{2\pi} e^{x \cos\theta} e^{\pm in\theta}, \quad [\text{evidently, } I_{-n}(x) = I_n(x)] \quad (23)$$

the above exact PDF given by (21) can be expressed in the closed form,

$$P_{\text{tag}}(X_t = \sigma_t z, r, t) = \frac{1}{\sigma_t} e^{-2\rho\sigma_t Q(z)} \left[ \frac{\sqrt{2Q(z) + z}}{\sqrt{2Q(z) - z}} \right]^r \\ \times \left\{ \left[ f(z) + 2\rho\sigma_t A_1(z)A_2(z) \right] I_r \left( \rho\sigma_t \sqrt{4Q^2(z) - z^2} \right) \right. \\ \left. + \rho\sigma_t A_1^2(z) \frac{\sqrt{2Q(z) + z}}{\sqrt{2Q(z) - z}} I_{r+1} \left( \rho\sigma_t \sqrt{4Q^2(z) - z^2} \right) \right. \\ \left. + \rho\sigma_t A_2^2(z) \frac{\sqrt{2Q(z) - z}}{\sqrt{2Q(z) + z}} I_{r-1} \left( \rho\sigma_t \sqrt{4Q^2(z) - z^2} \right) \right\}. \quad (24)$$

### 3. Large deviation result for the two-tags displacement

In this section, we obtain the large deviation form of (21) by evaluating the  $\theta$  integral using saddle point approximation. Note that in the expression of  $B(\theta, z)$  in (22), the second term is larger by  $O(\rho\sigma_t)$  compared to the first term  $f(z)$ , which comes from the process (i) where, in the non-interacting picture, the same particle happens to be the  $j^{\text{th}}$  and  $(j+r)^{\text{th}}$  particles at the initial and final times respectively. So this process does not contribute at  $O(\rho\sigma_t)$ .

In this case we also scale the final with  $\rho\sigma_t$ . The saddle point approximation of the integral in (21) gives

$$P_{\text{tag}}(X_t = \sigma_t z, r = \rho\sigma_t l, t) \approx \frac{1}{\sigma_t} \frac{\sqrt{\rho\sigma_t}}{\sqrt{2\pi g_2(z)}} g_1(z) e^{-\rho\sigma_t I(z)}, \quad (25)$$

where the different functions are explained below.

The large deviation function (rate function) is given by

$$I(z) = 2Q(z)(1 - \cos \theta^*) - iz \sin \theta^* + i\theta^* l, \quad (26)$$

where the saddle point  $\theta^*$  is obtained using the condition

$$\left. \frac{\partial}{\partial \theta} [2Q(z)(1 - \cos \theta) - iz \sin \theta + i\theta l] \right|_{\theta=\theta^*} = 0, \quad (27)$$

which gives

$$e^{\pm i\theta^*} = \frac{\pm l + \sqrt{l^2 + 4Q^2(z) - z^2}}{2Q(z) \pm z}. \quad (28)$$

Substituting  $\theta^*$  in (26) gives the large deviation function, explicitly in terms of  $z$  as

$$I(z) = 2Q(z) - \sqrt{l^2 + 4Q^2(z) - z^2} + l \ln \left[ \frac{l + \sqrt{l^2 + 4Q^2(z) - z^2}}{2Q(z) + z} \right]. \quad (29)$$

The function  $g_1(z)$  comes from evaluating the prefactor in (21) at the saddle point,

$$\begin{aligned} g_1(z) &= (\rho\sigma_t)^{-1} B(z, \theta^*) \\ &= \left[ 2A_1(z)A_2(z) + A_1^2(z)e^{-i\theta^*} + A_2^2(z)e^{i\theta^*} \right] + O([\rho\sigma_t]^{-1}), \end{aligned} \quad (30)$$

where  $e^{\pm i\theta^*}$  are given in (28).

The function  $g_2(z)$  comes from performing the Gaussian integral around the saddle-point  $\theta^*$ ,

$$g_2(z) = \left. \frac{\partial^2}{\partial \theta^2} [2Q(z)(1 - \cos \theta) - iz \sin \theta + i\theta l] \right|_{\theta=\theta^*} = \sqrt{l^2 + 4Q^2(z) - z^2}. \quad (31)$$

The large deviation function has a minimum at  $z = l$  and near this minimum, we get

$$I(z) = \frac{1}{2} \frac{(z - l)^2}{2Q(l)} + O([z - l]^3). \quad (32)$$

Therefore, near the peak at  $X_t = r/\rho$  the PDF  $P_{\text{tag}}(X_t, r, t)$  has a Gaussian form, which describes the *typical* fluctuations. However, away from this central region, the Gaussian approximation breaks down, and one require the large deviation result (25) to describe for the *atypical* large fluctuations. In figure 6 we compare both the Gaussian approximation and the large deviation result of the PDF with numerical simulation, and find that while the Gaussian approximation fits the data well near the central peak, the large deviation result agrees very well with the simulation data even beyond the central region.

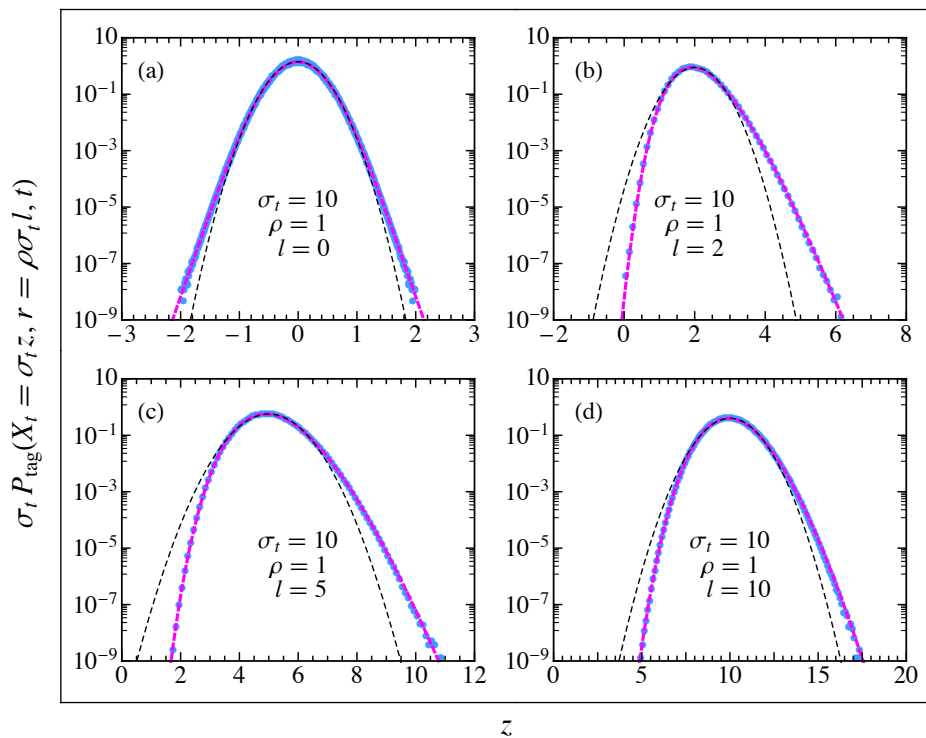


**Figure 6.** (Color online) The (blue) points represent the simulation results for the PDF of the two-tag displacement in a one-dimensional system of hard-point particles for tag separations (a)  $r = 0$ , (b)  $r = 20$ , (c)  $r = 50$ , and (d)  $r = 100$  respectively. The (magenta) thick dashed line corresponds to the analytic result in Eq. (25), while the (black) thin dashed line is for Gaussian distribution with the variance given by (37b).

#### 4. Cumulants

Now, we look at the cumulant generating function of the two-tag displacement  $X_t$ . We define

$$Z(\lambda) = \left\langle e^{\lambda \rho X_t} \right\rangle = e^{\rho \sigma_t \mu(\lambda)}, \quad (33)$$

such that the expansion of  $\mu(\lambda)$  in terms of the cumulants is given by

$$\mu(\lambda) = \frac{1}{\rho \sigma_t} \sum_{n=1}^{\infty} \frac{(\lambda \rho)^n}{n!} \langle X_t^n \rangle_c. \quad (34)$$

Using the large deviation form of  $P_{\text{tag}}(X_t, r, t)$  given by (25), and then evaluating the integral over  $z$  using the saddle point approximation, we have  $\mu(\lambda) = \lambda z^* - I(z^*)$  where  $z^*$  is implicitly given by the equation  $\lambda = dI(z^*)/dz^*$ . Using the expression of  $I(z)$  obtained above in terms of  $\theta^*$  with the substitution  $e^{-i\theta^*} = \nu$  we can express  $\mu(\lambda)$

in the parametric form

$$\mu(\lambda) = \lambda z + \frac{1-\nu}{1+\nu}(z+l) + l \ln \nu, \quad (35a)$$

$$\lambda = (1-\nu^{-1}) [1 + (\nu-1) A_1(z)], \quad (35b)$$

$$\nu = \frac{-l + \sqrt{l^2 + 4Q^2(z) - z^2}}{2Q(z) - z}. \quad (35c)$$

The absence of  $\rho$  and  $\sigma$  in (35) indicates that  $\mu(\lambda)$  does not depend on them. Therefore, from (34), it follows that

$$\langle X_t^n \rangle_c \propto \frac{\sigma_t}{\rho^{n-1}}. \quad (36)$$

Note that the above equations (35), obtained through the saddle point calculation, gives the cumulants only at the most dominant order  $O(\sigma_t)$ . To obtain the cumulants, we first expand the right hand side of (35c) about  $z = l$  and then invert the series to obtain  $z$  in terms of a series in  $\nu$  about  $\nu = 1$ . Therefore, the right hand side of (35b) can be expressed as a series in  $(\nu-1)$ . Next, by inverting (35b), we obtain  $\nu$  (and hence also  $z$ ) in terms of a series in  $\lambda$  about  $\lambda = 0$ . Finally, from (35a), we express  $\mu(\lambda)$  as a series in  $\lambda$ , and using the definition in (34), we obtain the first few cumulants (mean, variance, skewness, and kurtosis respectively) as

$$\sigma_t^{-1} \langle X_t \rangle_c = l, \quad (37a)$$

$$\sigma_t^{-1} \rho \langle X_t^2 \rangle_c = 2Q(l) \quad (37b)$$

$$\sigma_t^{-1} \rho^2 \langle X_t^3 \rangle_c = 12F(l)Q(l) - l, \quad (37c)$$

$$\sigma_t^{-1} \rho^3 \langle X_t^4 \rangle_c = 6 \left[ 8f(l)Q^2(l) - Q(l) + 20F^2(l)Q(l) - 2lF(l) \right], \quad (37d)$$

where  $l = r/(\rho\sigma_t)$  and  $F(l) = \int_0^l f(w) dw$ .

While the mean  $\langle X_t \rangle_c = r/\rho$  is exact to all order, the expressions for the other three cumulants are exact only at the leading order  $O(\sigma_t)$ . The sub-dominant corrections can be computed using the exact expression of the PDF given by (21). For example, for the variance we get

$$\begin{aligned} \langle X_t^2 \rangle_c = \frac{1}{\rho^2} & \left\{ 2\rho\sigma_t Q(l) + \left[ 2f(l)Q(l) + 2F^2(l) - \frac{1}{2} \right] \right. \\ & + [\rho\sigma_t]^{-1} \left[ Q^2(l)f''(l) + f'(l) \left( 8F(l)Q(l) - \frac{l}{3} \right) + f(l) \left( 12F^2(l) - 1 \right) + 6f^2(l)Q(l) \right] \\ & \left. + O([\rho\sigma_t]^{-2}) \right\}. \end{aligned} \quad (38)$$

## 5. Velocity autocorrelations

As a spin-off of our calculation, we show here that for the Hamiltonian model of elastically colliding particles, we can also compute the velocity auto-correlation function

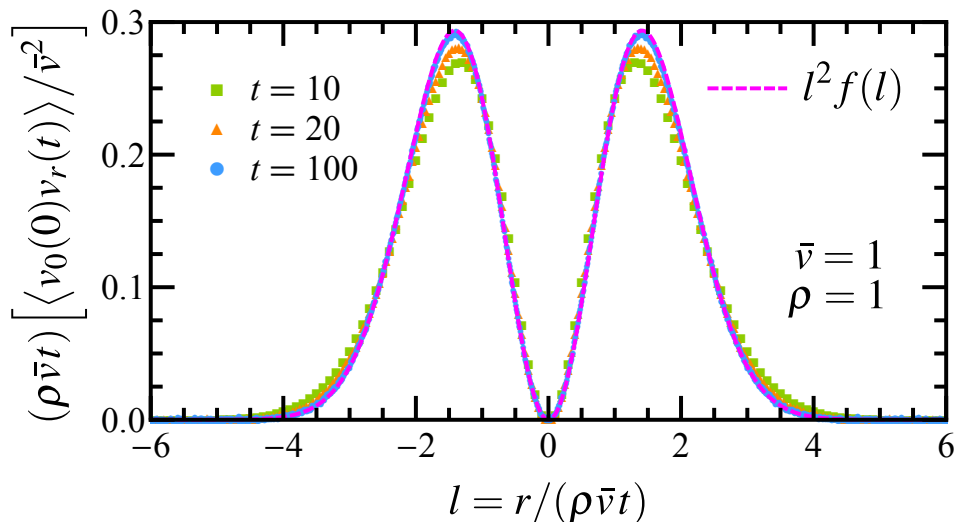


**Figure 7.** The points are numerical simulation results for the velocity auto-correlation function computed from two tagged particles as a function of the tag separation at three different times, for the Hamiltonian model. The dashed line represent the analytical result to the leading order.

$\langle v_0(0)v_r(t) \rangle$ . This can in fact be derived directly from the positional correlation function. We note that for the Hamiltonian case, we have  $x_i(t) = \int_0^t dt' v_i(t')$ . Hence it follows that

$$\frac{1}{2} \frac{d}{dt} \langle [x_r(t) - x_0(0)]^2 \rangle = \frac{1}{2} \frac{d}{dt} \left[ \langle x_r^2(t) \rangle + \langle x_0^2(0) \rangle - 2 \langle x_r(t)x_0(0) \rangle \right]. \quad (39)$$

The first two terms inside the square bracket are independent of time, hence they drop off on taking a time-derivative. For a Hamiltonian system we have  $(d/dt) \langle x_r(t)x_0(0) \rangle = \langle v_r(t)x_0(0) \rangle = \langle v_r(0)x_0(-t) \rangle$ . Taking another derivative, we get

$$\frac{1}{2} \frac{d^2}{dt^2} \langle [x_r(t) - x_0(0)]^2 \rangle = \langle v_r(t)v_0(0) \rangle. \quad (40)$$

Using Eq. (38), the fact that  $d^2Q/dl^2 = f(l)$ , and  $\sigma_t = \bar{v}t$  for Hamiltonian dynamics, we therefore get

$$\frac{1}{\bar{v}^2} \langle v_r(t)v_0(0) \rangle = \frac{1}{2} \frac{d^2}{d\sigma_t^2} \langle X_t^2 \rangle_c \quad (41)$$

$$= \frac{1}{\rho\sigma_t} l^2 f(l) + O([\rho\sigma_t]^{-2}). \quad (42)$$

To leading order, this result can be obtained by a simple argument. Since the initial velocities are chosen independently for each particle, the contribution to the correlation function  $\langle v_r(t)v_0(0) \rangle$  is non-zero only when the velocity of the  $r$ -th particle at time  $t$  is

the same as that of the zero-th particle at time  $t$ . Thus we have

$$\begin{aligned} \langle v_0(0)v_r(t) \rangle &\simeq \langle \delta(r - \rho vt) v^2 \rangle = \frac{1}{\rho t} \left\langle \delta \left( v - \frac{r}{\rho t} \right) v^2 \right\rangle \\ &= \frac{1}{\rho t} \int \delta \left( v - \frac{r}{\rho t} \right) v^2 \frac{1}{\bar{v}} f \left( \frac{v}{\bar{v}} \right) dv, \end{aligned} \quad (43)$$

hence finally

$$\frac{1}{\bar{v}^2} \langle v_0(0)v_r(t) \rangle \simeq \frac{1}{\rho \bar{v} t} \left( \frac{r}{\rho \bar{v} t} \right)^2 f \left( \frac{r}{\rho \bar{v} t} \right), \quad (44)$$

as in Eq. (42). In figure 7 we show a comparison of this analytic result with direct simulation results for the two-particle velocity autocorrelations in the equilibrium hard-particle gas. An exact expression for the velocity autocorrelation was obtained in [1] and involves a very lengthy calculation. This exact result can be recovered from using Eqs. (24,41). However we see that the leading order expression is already quite accurate in describing the long time behavior. For the special case  $r = 0$  and equilibrium initial conditions, using (38) in (41), we get

$$\frac{1}{\bar{v}^2} \langle v_0(0)v_r(t) \rangle \simeq (\rho \bar{v} t)^{-3} \left[ Q^2(0) f''(0) - f(0) + 6Q(0) f^2(0) \right]. \quad (45)$$

For the Gaussian distribution,  $f(x) = \exp(-x^2/2)/\sqrt{2\pi}$ , this gives  $\langle v_0(t)v_0(0) \rangle/\bar{v}^2 \simeq -(\rho \bar{v} t)^{-3} (2\pi - 5)/(2\pi)^{3/2}$ , a result first derived in [1], and also in [16] using the present approach.

## 6. Discussion

We have considered a system of point particles moving on a one-dimensional line. The dynamics of individual particles is arbitrary and can be either stochastic or deterministic, and the only interaction between the particles is when they meet. The interaction dynamics is specified by imposing that, we start with the non-interacting trajectories, and then interchange particle labels whenever trajectories cross — thus the ordering of particle labels is maintained at all times. This dynamics is quite natural for the deterministic so-called Jepsen gas and also for non-crossing Brownian walkers, and also seems natural for other stochastic processes. Using the fact that a mapping to non-interacting particles is available we have developed a formalism that seems to be very suited to computing reduced distribution functions and correlation functions in the interacting system. In particular, here we focus on computing the joint distribution of the positions of two tagged particles at different times. This is obtained exactly and from this we extract the large deviation function, various cumulants. For the case of Hamiltonian dynamics, we show that the two-pont velocity autocorrelation function can also be computed. We expect that the general strategy of our approach will be useful in the computation of more complicated correlations and distribution functions.

## 7. Acknowledgments

We thank the Galileo Galilei Institute for Theoretical Physics for the hospitality and the INFN for partial support during the completion of this work.

- [1] D. W. Jepsen, *J. Math. Phys.* **6**, 405 (1965).
- [2] T.E. Harris, *J. Appl. Probab.* **2**, 323 (1965).
- [3] J. L. Lebowitz and J. K. Percus, *Phys. Rev.* **155**, 122 (1967).
- [4] J. L. Lebowitz and J. Sykes, *J. Stat. Phys.* **6**, 157 (1972).
- [5] J. K. Percus, *Phys. Rev. A* **9**, 557 (1974).
- [6] H.van Beijeren, K.W. Kehr, and R. Kutner, *Phys. Rev. B* **28**, 5711 (1983).
- [7] R. Arratia, *Ann. Probab.* **11**, 362 (1983).
- [8] S. Alexander and P. Pincus, *Phys. Rev. B* **18**, 2011 (1978).
- [9] C. Rödenbeck, J. Kärger, and K. Hahn, *Phys. Rev. E* **57**, 4382 (1998).
- [10] S. N. Majumdar and M. Barma, *Phys. Rev. B* **44**, 5306 (1991).
- [11] L. Lizana and T. Ambjörnsson, *Phys. Rev. Lett* **100**, 200601 (2008); *Phys. Rev. E* **80**, 051103 (2009).
- [12] E. Barkai and R. Silbey, *Phys. Rev. Lett.* **102**, 050602 (2009).
- [13] M. Kollmann, *Phys. Rev. Lett.* **90**, 180602 (2003).
- [14] S. Gupta, S. N. Majumdar, C. Godrèche and M. Barma, *Phys. Rev. E* **76**, 021112 (2007).
- [15] E. Barkai and R. Silbey, *Phys. Rev. E* **81**, 041129 (2010).
- [16] A. Roy, O. Narayan, A. Dhar and S. Sabhapandit, *J. Stat. Phys.* **150**, 851 (2013).
- [17] A. Roy, A. Dhar, O. Narayan and S. Sabhapandit, *J. Stat. Phys.* (2015).
- [18] S. Sabhapandit, *J. Stat. Mech.* **L05002** (2007).
- [19] P. Illien *et al.*, *Phys. Rev. Lett.* **111**, 038102 (2013).
- [20] O. Bénichou *et al.*, *Phys. Rev. Lett.* **111**, 260601 (2013).
- [21] P. L. Krapivsky, K. Mallick, and T. Sadhu, *Phys. Rev. Lett.* **113**, 078101 (2014).
- [22] C. Hegde, S. Sabhapandit, and A. Dhar, *Phys. Rev. Lett.* **113**, 120601 (2014).
- [23] P. L. Krapivsky, K. Mallick, and T. Sadhu, arXiv:1505.01287.
- [24] T. Sadhu and B. Derrida, arXiv:1505.04572.
- [25] K. Damle and S. Sachdev, *Phys. Rev. Lett.* **95**, 187201 (2005).
- [26] Á. Rapp and G. Zaránd, *Phys. Rev. B* **74**, 014433 (2006).